

# Study of the composition, structure, and effect of water absorption on the wall of bovine hooves from the Brazilian Northeast region

Wendell Bruno Almeida Bezerra<sup>1\*</sup>, Ulisses Oliveira Costa<sup>1</sup>, Fabio da Costa Garcia Filho<sup>1</sup>, Sergio Neves Monteiro<sup>1</sup>  
<sup>1</sup>Instituto Militar de Engenharia (IME).

Praça General Tibúrcio, 80, 22290-270, Praia Vermelha, Rio de Janeiro, RJ, Brasil,  
\*wendellbez@ime.eb.br

**ABSTRACT:** Over thousands of years natural materials have evolved to complex and multifunctional hierarchical structures. An example of this, bovine hooves are keratinous materials differentiated from other types of hooves whose structure and composition are not yet as well-known as that of equine hooves. Thus, the present work aimed to investigate the influence of absorbed water on the structure and composition of bovine hooves from the Northeast region of Brazil. The hulls were evaluated using X-ray diffraction analysis (XRD), Fourier transform infrared spectroscopy (FTIR) and scanning electron microscopy (SEM). The effect of water on the amorphous keratin matrix of the hooves can be observed through DRX and FTIR analyses, as well as identifying different zones and dimensions of the tubules in the structure through SEM images. The results present a starting point for the correlation between structure and impact absorption mechanisms in these materials.

**KEYWORDS:** Keratin. Bovine hooves. Water absorption. Composition. Structure.

**RESUMO:** Ao longo de milhares de anos, os materiais naturais evoluíram, desenvolvendo estruturas hierárquicas complexas e multifuncionais. Um exemplo disso, os cascos bovinos, são materiais queratinosos diferenciados de outros tipos de cascos cuja estrutura e composição ainda não são tão conhecidas como a dos cascos equinos. Dessa forma, o presente trabalho se propôs a investigar a influência da água absorvida na estrutura e composição de cascos bovinos oriundos da região Nordeste do Brasil. Os cascos foram avaliados através de análises de difração de raios X (DRX), espectroscopia no infravermelho por transformada de Fourier (FTIR) e microscopia eletrônica de varredura (MEV). Pode-se observar o efeito da água na matriz de queratina amorfa dos cascos através das análises de DRX e FTIR, bem como identificar diferentes zonas e dimensões dos túbulos na estrutura através das imagens de MEV. Os resultados apresentam um ponto de partida para a correlação entre a estrutura e os mecanismos de absorção de impacto nesses materiais.

**PALAVRAS-CHAVE:** Queratina. Cascos bovinos. Absorção de água. Composição. Estrutura.

## 1. Introduction

Many biological materials have evolved in such a way as to have multifunctional structures and the ability to absorb considerable amounts of energy without fracturing. These include functions such as protection (e.g. mollusc shells, bones), defense and aggression (e.g. claws, teeth, fangs, horns and antlers), support (e.g. bones, mollusc shells and hooves) and chewing (e.g. teeth) [1]. These materials are made up of different structural components with different chemical and physical characteristics [2]. Notable among these are keratin-based components [3].

Keratin is made up of polypeptide chains. This component has variants that can be found both in mammals,

constituting hair, nails, hooves, horns and the epidermal layer of the skin, and in reptiles and birds, in their claws, scales, feathers and beaks [4]. Initially, some of these materials attracted the most interest because of their ability to absorb a considerable amount of energy and resist impact (e.g. hooves and horns) [1, 3-5].

Keratins can be classified as types  $\alpha$  and  $\beta$ . Both have a matrix-filament type structure, observed in each type in the form of: intermediate filaments (IFs) 7 nm in diameter in the case of  $\alpha$ -keratin, and filaments 3 nm in diameter in  $\beta$ -keratin, both embedded in an amorphous keratin matrix. [4]. In this sense, water plays a fundamental role in the mechanical properties of structural biological materials. Similarly, the mechanical properties of  $\alpha$ -keratin and  $\beta$ -keratin are influenced by water content.

In general, the presence of water defines the structural characteristics and physical properties of proteins and organic substances, acting as a plasticizer in biological materials, increasing their ductility and decreasing their toughness. In this way, without water, biological materials lose their original mechanical properties and become more fragile [2]. The same occurs with keratin: as humidity increases, stiffness and strength decrease, while tensile strength increases [4].

Through X-ray diffraction and experimental studies, previous works have revealed that matrix proteins can be considered to be sensitive to water, while IFs are crystalline and are not mechanically affected by humidity [6-10]. In general, this can be extended to keratinous materials, since IFs do not change in the different rigid keratins of mammals [6]. Different models have been proposed to explain how the interaction between water molecules and matrix proteins occurs.

According to the proposed models:

- a. Water can act as a swelling agent, forming a cross-link with the chains, resulting in a reduction in the interaction between the chains and an increase in the intermolecular space [10];
- b. Water can break/replace secondary bonds present between glycine/tyrosine-rich proteins in the matrix phase, such as hydrogen bonds, resulting in greater protein mobility [7,9];
- c. Water can form a three-dimensional keratin-water molecule network that acts as a plasticizer, resulting in less rigidity and greater segmental mobility of the matrix's molecular structure [6,10].

Keratinous biological materials, which have different structures with keratin as their main component, have their properties directly linked to the sensitivity of this component. When dehydrated, these materials lose their original mechanical properties and become more fragile. Therefore, in order to correctly assess the mechanical properties of biological materials, it is extremely important to take into account the degree of hydration [2].

However, before we can apply biological structures to the manufacture of bioinspired materials, we need a thorough understanding of the relationship between

structure and properties in these complex materials. Several studies have focused on this paradigm, in particular equine hooves and American wild sheep horns [5, 11,12]. In addition to these, some materials from other species have had their structures and properties analyzed, such as bovine hooves [13-16], but little focus is applied to the relationship between structure and dynamic behavior.

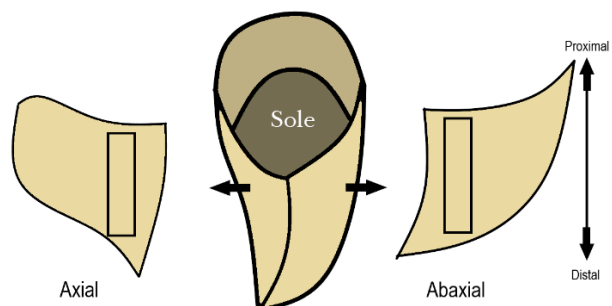
Based on the literature, the analysis of these characteristics in keratinous biological materials is proving useful in the development of bio-inspired systems and structures which are expected to perform better with subsequent improvements in materials processing and production technology.

The aim of this work is to study the relationship between composition, structure and the effect of water on keratinous biological materials, such as bovine hooves, in order to provide a starting point for the development of new bioinspired impact-resistant materials.

## 2. Materials and methods

The hooves of bovine species from northeastern Brazil were studied to analyze their composition and structure. The hooves of different animals were obtained from the municipal slaughterhouse in the city of Juazeiro do Norte, Ceará. The hooves were washed and then left to dry at room temperature, without specific humidity control. Figure 1 shows the bovine hoof with its respective anatomical regions, taken into account when preparing the samples.

**Fig. 1** - Anatomical positions of the hooves and sampling regions. Source: Author.



## 2.1 Water absorption

In order to assess the time required for the hooves to fully hydrate after immersion, water absorption tests were carried out. As there is no specific standard for natural materials, the tests were based on ASTM D570-98 (2018). Five (5) samples were prepared from two different regions of the abaxial wall of bovine hooves, thus characterizing two groups: abaxial-proximal (AB-P) and abaxial-distal (AB-D). The samples were weighed and immersed in deionized water and re-weighed after immersion periods of: five (5min), ten (10min), twenty (20min) and thirty (30min) minutes, and one (1h), two (2h), three (3h), four (4h), twenty-four (24h), forty-eight (48h), seventy-two (72h) and ninety-six (96h) hours. After the final immersion time, the samples were separated, weighed and their moisture content assessed, as described in previous studies [14,16]. The samples were then placed in an oven at 70°C for a period of seven (7) days. The moisture content (MC %) can be determined using Equation 1:

$$MC \% = \frac{\text{wet mass} - \text{dry mass}}{\text{wet mass}} \times 100\% \quad (1)$$

## 2.1 X-ray diffraction (XRD)

The samples were prepared from two different regions of the abaxial wall, namely abaxial-proximal (AB-P) and abaxial-distal (AB-D). One sample from each group was subjected to each of the two different hydration conditions: conditioned at room temperature (AD) and fully hydrated (100). In addition, the inner (IW) and outer (EW) wall surfaces were evaluated on the AB-D sample. Thus, the samples were named according to Table 1.

The analyses were carried out on an X-ray diffractometer, model X'Pert Pro Panalytical, available from the Military Engineering Institute (IME), using a CoK $\alpha$  radiation source (1.790307 Å). The parameters used were: 40 kV voltage, 40 mA current, 0.04 degree step. The spectra were obtained for values of 2 $\theta$  from 5 to 50°, based on the literature found [18,19].

Using OriginPro 2019 software, the data obtained was subjected to noise removal using the Savitzky-Golay method, and the curves were adjusted with deconvolution of the halos in order to determine the position of the peaks more precisely.

**Tab. 1** - Nomenclature of samples for XRD analysis under the different conditions studied

Region	Hydration	Surface	Nomenclature
Abaxial-distal (AB-D)	AD	External (EW)	<b>AB-D-AD-EW</b>
		Internal (IW)	<b>AB-D-AD-IW</b>
	100	External (EW)	<b>AB-D-100-EW</b>
		Internal (IW)	<b>AB-D-100-IW</b>
Abaxial-proximal (AB-P)	AD	External	<b>AB-P-AD</b>
	100	-	<b>AB-P-100</b>

**Source:** Author

## 2.2 Fourier transform infrared spectroscopy (FTIR)

In order to better understand the effect of hydration on the chemical structure of the hoof components, Fourier transform infrared spectroscopy (FTIR) analyses were carried out with different

sample conditions. These were prepared from two different regions of the abaxial wall, called abaxial-proximal (AB-P) and abaxial-distal (AB-D). From each group of regions, two hydration conditions were prepared: drying at room temperature (sa) and fully hydrated (100).

The analyses were carried out on a PerkinElmer Frontier FT-IR/FIR device, in transmittance mode with KBr pellets, with a resolution of  $4\text{ cm}^{-1}$ , using a wave number range of  $4,000$  to  $400\text{ cm}^{-1}$ . The transmittance mode using KBr pellets was chosen in order to compare the spectra obtained with those reported for other keratinous materials and hoof keratin membranes [18,19].

### 2.3 Scanning electron microscopy (SEM)

In order to characterize the surface morphology of the hoof wall and its internal structure, scanning electron microscopy (SEM) analyses were carried out. Since the materials are not electrically conductive, they were subjected to a metallic surface coating using LEICA equipment, model EM ACE600, and the analyses were carried out on FEI equipment, model Quanta FEG 250, both available at the IME.

## 3. Results and discussion

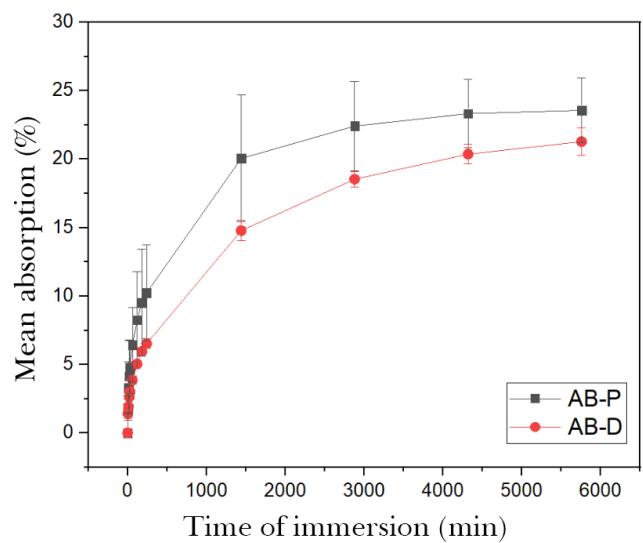
### 3.1 Water absorption

Moisture content is known to be one of the factors affecting the mechanical properties of structural biological materials, especially hoof walls [14]. Therefore, in order to speed up the procedure for preparing samples for future work, water absorption tests were carried out on two different regions of the abaxial wall of bovine hooves.

Figure 2 shows the mean percentage increases in weight observed in the samples after the proposed immersion time intervals. Accelerated absorption was observed in the first few minutes with a subsequent reduction in the absorption rate, due to water saturation in the structure of the material [20]. Similar behavior has been observed in other structural biological materials [9,21]. In addition, it is possible to observe an asymptotic tendency of the points to plateau after three days (4,320 min) of immersion. In the case of oryx horns, Kitchener (1987) reports the total hydration of the material, represented by the plateau, after 3 days, while for equine hooves, complete hydration occurs after 5 days [9].

Despite the apparent trend for the abaxial-proximal wall to absorb more on average, no significant differences were observed between the two regions. After four days of immersion (5,760 min), mean values of  $23.58 \pm 2.37\%$  were observed for the abaxial-proximal region (AB-P) and  $21.28 \pm 1.00\%$  for the abaxial-distal region (AB-D).

**Fig. 2** - Mean water absorption (%) for each region of the abaxial wall of bovine hooves: proximal and distal.



Previous works have studied the effect of atmospheric relative humidity on the moisture content of different hooves, especially single-digit hooves such as those of horses and donkeys [9,22]. In both cases, the curves of moisture content versus atmospheric relative humidity show an exponential increase in the level of hoof hydration with the increase in ambient relative humidity.

Baillie and colleagues (2000) proposed that the best way to simulate the levels of hydration present in hooves *in vivo* would be through immersion in an aqueous medium. In this way, it is expected that, due to the presence of tubules in the internal structure of the wall, there will be a direct effect of capillarity on the hydration obtained. However, in equine hooves, the formation of hydration gradients (*i.e.* greater hydration in the distal region) expected for this case was not observed [20]. On the contrary, a higher rate

of dehydration was observed in the distal region due to the presence of openings in the tubules.

The mean values and the respective standard deviations of the moisture contents obtained for the samples from the two groups studied are shown in the Table 2. In the literature, values can be found for bovine hooves ranging from 3.11 to 35.50 %w/w H<sub>2</sub>O, depending on the hydration or dehydration conditions used [14,16]. The values found in this

study are very close to those reported by Wang et al. (2020), of 28.05 and 27.15%. In addition, a significant difference (*i.e.* confidence interval = 95%) was observed in the moisture content values of the two regions studied, which is similar to that reported for equine hooves [9]. The moisture content of hooves dried at ambient humidity (AD) was 10.03 and 11.32% for the abaxial-distal (AB-D) and abaxial-proximal (AB-P) regions, respectively.

**Tab. 2 - Mean moisture content of samples after hydration**

Sample	Mean moisture content (%w/w H <sub>2</sub> O)	Standard deviation
AB-P-100	25.05	1.50
AB-D-100	22.52	0.80

### 3.2 X-ray diffraction (XRD)

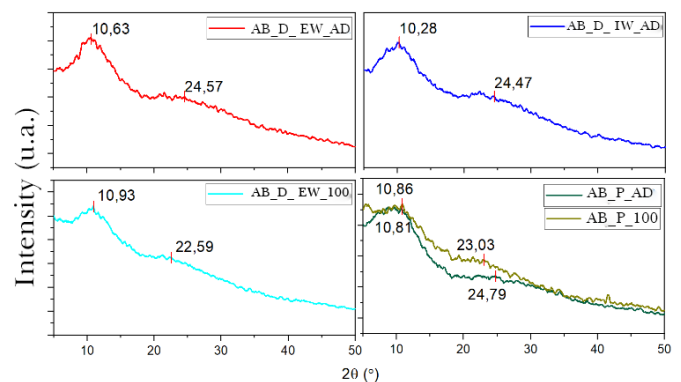
The physical structure of keratins has been studied for a long time and is widely reported in the literature [4,8]. Through X-ray diffraction it is possible to identify three characteristic patterns:  $\alpha$  pattern,  $\beta$  pattern and feather pattern, in addition to the amorphous pattern. In most mammals, the keratin found shows the  $\alpha$  pattern [4], exhibiting two typical spacings: one related to the distance between the molecules that make up the  $\alpha$ -helix, of 9.80 Å, and the other related to the step between the two molecules of the  $\alpha$ -helix, of 5.15 Å [23].

The diffractograms obtained for the samples of the abaxial wall of the bovine hoof, from the proximal and distal regions under the two hydration conditions, are shown in Figure 3. By fitting the curves, it was possible to observe two characteristic halos in the different samples. The presence of halos rather than peaks is associated both with the fact that the hoof wall has an amorphous keratin matrix and with the fact that the intermediate filaments (IFs) have a crystallinity order at the nanometric level.

The first halo was found at Bragg angles ( $2\theta$ ) ranging from 10.28 and 10.93°. From these values, the interplanar spacings could be identified, as shown in 3, resulting in a mean spacing of  $9.60 \pm 0.24$  Å. No significant variation was identified between the structure

of the inner (AB\_D\_PI\_AD) and outer (AB\_D\_PE\_AD) hoof walls, or between the distal and proximal regions. The second halo was found at Bragg angles ( $2\theta$ ) of 22.59 to 24.79°. The spacings related to these angles are shown in Table 3. A mean spacing of  $4.33 \pm 0.18$  Å was observed, very close to that reported for other keratinous materials, as shown in the same table.

**Fig. 3 - Diffractograms obtained for samples from different regions of the hoof and under different hydration conditions.**



In order to avoid the inherent variability of natural materials, the same samples were evaluated in both hydration conditions, air-dried (AD) and immersed (100). In this way, comparing the two conditions allowed a better understanding of the influence of hydra-

tion on the physical structure of the hooves. There was a slight trend for the spacing related to the first halo to decrease: from 9.66 to 9.40 Å in the distal region (AB\_D), and from 9.50 to 9.46 Å in the proximal region. Conversely, an upward trend was observed in the spacing related to the second halo: from 4.21 to 4.57 Å in the distal region (AB\_D), and from 4.17 to 4.48 Å in the proximal region.

It is believed that these halos are directly associated with the spacings reported for the  $\alpha$ -helix structure of keratin [8,19]. The findings reinforce the theory that water molecules can replace secondary bonds, such as hydrogen bonds, present between glycine/tyrosine-rich proteins in the matrix phase [7,9]. The introduction of water molecules into the structure generates an increase in the  $\alpha$ -helix step distance, resulting in an increase in the spacings observed in both regions in the second halo, which suggests a decrease in the packing of the keratin crystal structure in the IFs.

**Tab. 3** - Interplanar spacing of the samples analyzed in this study and keratinous materials reported in the literature

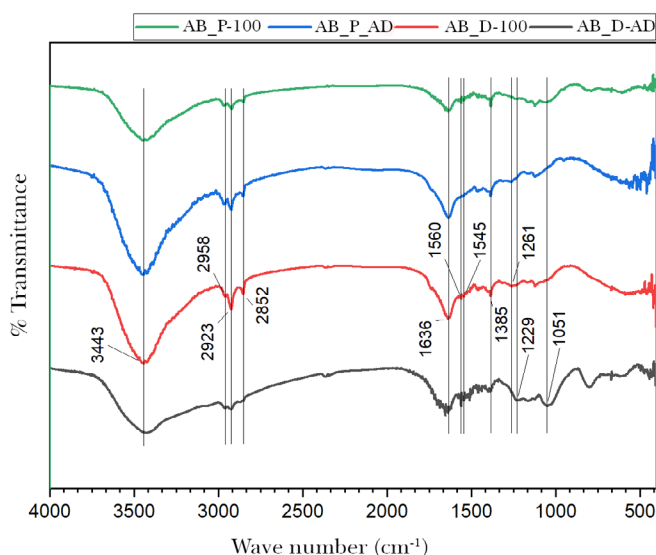
Material	d (Å)	Reference
AB_D_EW_AD	4.21	Present work (PW)
	9.66	
AB_D_IW_AD	4.22	
	9.99	
AB_D_EW_100	4.57	
	9.40	
AB_P_AD	4.17	
	9.50	
AB_P_100	4.48	
	9.46	
Wool	4.35	Wu and colleagues (2017)
Pure keratin	4.46	
Bovine hoof keratin	4.62	Valkov and colleagues (2020)

Material	d (Å)	Reference
Hair keratin	4.48	Valkov and colleagues (2020)
Nail keratin	4.27	
$\alpha$ -keratin standard	5.15	Fraser, MacRae and Rogers (1972)
	9.80	

### 3.3 Fourier transform infrared spectroscopy (FTIR)

The composition of the bovine hoof wall and the effect of hydration on it can be assessed by studying the structure of the molecules that make up the material using infrared spectroscopy. The spectra obtained for the samples extracted from the proximal and distal regions of the abaxial hoof wall in the two hydration conditions, dry and hydrated, are shown in Figure 4. The presence of bands common to all the samples can be seen, with greater or lesser associated transmittance intensity. Of particular note are the bands found at frequencies between 3,600 and 3,200  $\text{cm}^{-1}$ , related to N-H and O-H stretching vibrations; between 2,958 and 2,852  $\text{cm}^{-1}$ , referring to C-H stretching vibrations; and 1,636  $\text{cm}^{-1}$ , associated with the C=O and C-N stretching vibrations present in amides I [19].

**Fig. 4** - Infrared spectra of the samples extracted from the different regions of the abaxial wall of bovine hooves, under the different hydration conditions studied



In addition, bands were observed at 1,560 and 1,545  $\text{cm}^{-1}$  which are associated with the N-H angular deformation and C-N and C-C stretching vibration modes of amide II [19,24]. Table 4 summarizes the frequencies related to the main bands observed, the associated vibration modes and the values reported in the literature for other keratin structures.

The main difference observed between the proximal and distal regions of the hoof wall is related to the intensity of the band present at 1.051  $\text{cm}^{-1}$ . This band is associated with the S-C bonds present in the cysteine that makes up keratin [24]. It is therefore believed that the greater intensity of the band observed in the distal region may be associated with a greater quantity of this amino acid in the structure.

In relation to the hydration condition, it was possible to observe a considerable increase in the

intensity of the O-H band at 3.443  $\text{cm}^{-1}$ , which is directly related to the level of humidity of the samples [19]. In addition, looking at the ratio between the intensities of the characteristic C=O and N-H bands, we can see a decrease in the intensity of the latter in relation to the former as the moisture content of the samples increases [25]. It is also possible to observe a change in the intensity ratio of the bands at 1,636 and 3,443  $\text{cm}^{-1}$ , after the samples were hydrated. The higher intensity of the 1,636  $\text{cm}^{-1}$  band observed in the hydrated samples may be associated with the more frequent occurrence of hydrogen bonds [26]. In the case of wild sheep horn [25], a variation in the position of the bands was also reported which was associated with an increase in moisture content, but this phenomenon was not observed in the present study.

**Tab. 4 -** Frequencies of the absorption bands observed in the samples studied and in other keratinous materials studied in the literature.

Material	Type of vibration	Wave number ( $\text{cm}^{-1}$ )	Ref.
Bovine hoof wall	N-H and O-H stretching	3.600-3.200	Author
	C-H stretching	2.958-2.852	
	C=O and C-N stretching of amides I	1.636	
	N-H angular deformation and C-N and C-C stretching of amides II	1.560-1.530	
	Angular deformation of C-H and stretching of $-\text{CH}_3$	1.385	
	C-N stretching and C=O angular deformation of amides III	1.260-1.230	
Goat hoof keratin	Characteristic of cysteine	1.070-1.040	[27]
	N-H and O-H stretching	3.650-3.250	
	Characteristic of amides I	1.665-1.610	
Bovine hoof keratin	Characteristic of amides II	1.550-1.520	[19]
	N-H stretching of amides A and O-H hydration	3.355-3.295	
	C=O and C-N stretching of amides I	1.650	
	N-H angular deformation and C-N and C-C stretching of amides II	1.530	
	C-N stretching and C=O angular deformation of amides III	1.230	

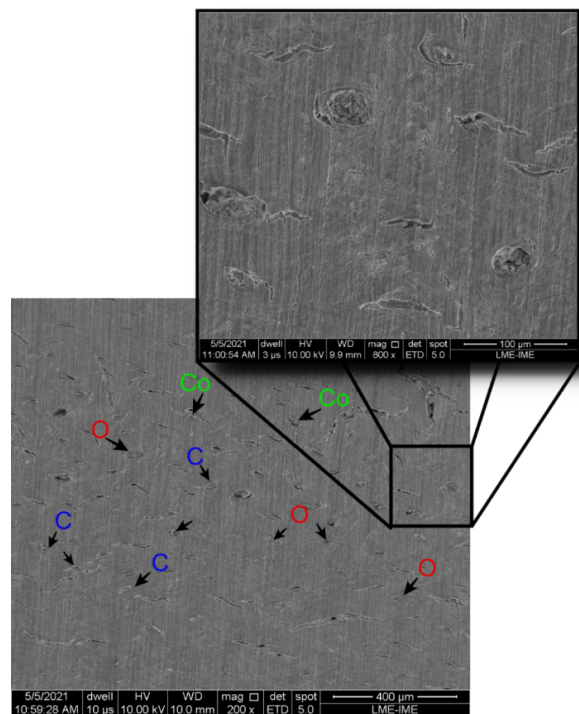
Material	Type of vibration	Wave number (cm <sup>-1</sup> )	Ref.
Goat hoof wall	N-H and O-H stretching	3.400	[24]
	C-H stretching	2.960-2.870	
	CO stretching of amides I	1.655	
	CN stretching and NH angular deformation of amides II	1.540-1.520	
	Angular deformation of C-H and stretching of -CH <sub>3</sub>	1.387	
	CN stretching and NH angular deformation of amides III	1.238	
	Characteristic of -S-C	1.051	
Characteristic of S=O	1.076		

### 3.4 Scanning electron microscopy (SEM)

In order to better understand the internal structure of the material, samples from different regions of the abaxial wall of bovine hooves were studied using scanning electron microscopy (SEM). The sanded samples from the distal, intermediate and abaxial regions of the hooves were observed and their micrographs are presented below.

Figure 5 shows micrographs taken at different magnifications of the cross-section of the proximal region of the bovine hoof wall. It is possible to see the opening of the tubule structure, some of which are selected and indicated by arrows. This structure is well known and has been reported in various keratinous materials, including bovine hooves [4,14,16,28-30]. One of the important factors to consider is the quantity of these components present in a given area, known as tubule density (mm<sup>-2</sup>). The importance of this factor is mainly associated with the moisture content of the material, since the lower the tubule density, the greater the amount of intertubular material and, consequently, the higher the moisture content [28]. Figure 5 also shows tubules with various shapes, such as circular, oval and collapsed, similar to what has been reported in the literature [29].

**Fig. 5** - Micrograph of the cross-section of the hoof wall in the proximal region, showing the presence of circular (C), oval (O), collapsed (Co) tubules and cracks in the intertubular material.



In all the regions studied, four distinct zones could be identified: lamellar, in the inner wall; internal; inter-

mediate, divided into two others with different tubule shapes and keratinocyte orientations; and external, with collapsed tubules. This division is well known and reported in the literature, but there is little information on the orientation of the keratinocytes in the intertubular matrix. Figure 6 shows the wall in total, with the lamellar zone highlighted by the square, 1.49  $\mu\text{m}$  long in the distal region. The arrows indicate the orientation of the intertubular material, which could be identified by the direction of the cracks resulting from cutting the samples. In the case of equine hooves, the cracks follow the orientation of the contours of the keratin cells in the intertubular material [5]. This phenomenon also seems to occur in the bovine hooves studied here, as illustrated by the direction of the arrows. In this way, the internal zone can be identified, found immediately after the lamellar zone and characterized by the absence of tubules, followed by an intermediate region subdivided by the different orientations of the IFs [14,30]. The fourth and final zone is closest to the outer wall and appears to have mostly collapsed tubules.

**Fig. 6** - Micrograph of the cross-section of the hoof wall in the distal region, showing the four zones observed along the wall and the orientation directions of the IFs in the intertubular material.

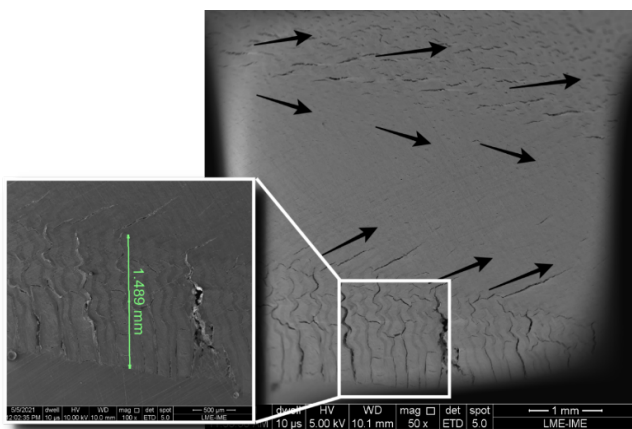
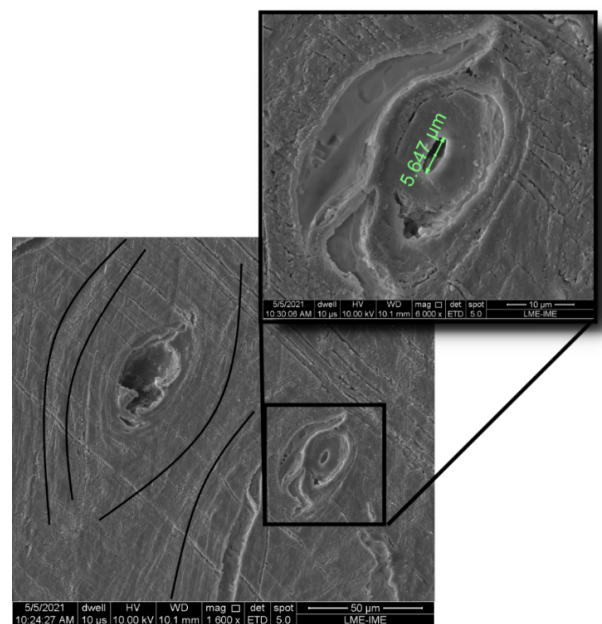


Figure 7 shows a micrograph of the cross-section of the hoof wall in the intermediate region, between the distal and proximal regions. It is possible to see two adjacent tubules with apparently different diameters, but elliptical in shape. Due to the rather irregular shape of

the tubule on the left, it is believed that the central region of the tubule was torn off during sample preparation. The figure also shows the interface present in the intertubular material between what would be the two keratin cells. The proposed layered structure of the tubules can be seen in the delamination observed in the magnified region of Figure 7, which shows the diameter of the tubule (*i.e.* 5.65  $\mu\text{m}$ ). One can clearly see the separation of the layers adjacent to the tubule lumen, with a small bundle of intertubular material joining the layers.

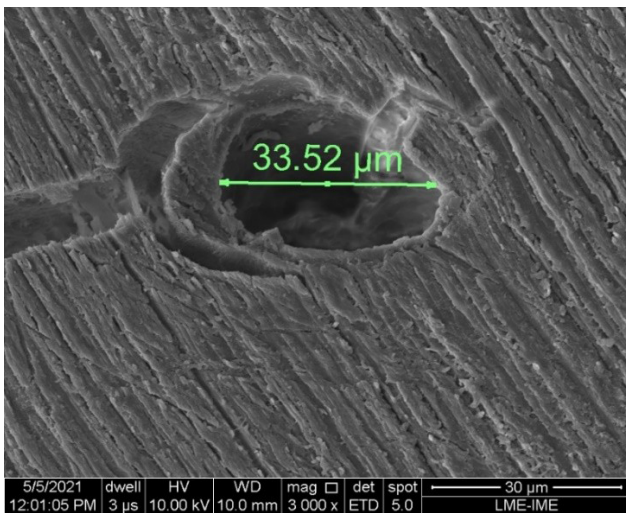
**Fig. 7** - Micrograph of the cross-section of the hoof wall in the intermediate region, showing the interface region between the keratin cells and the dimensions of one of the tubules observed in this region.



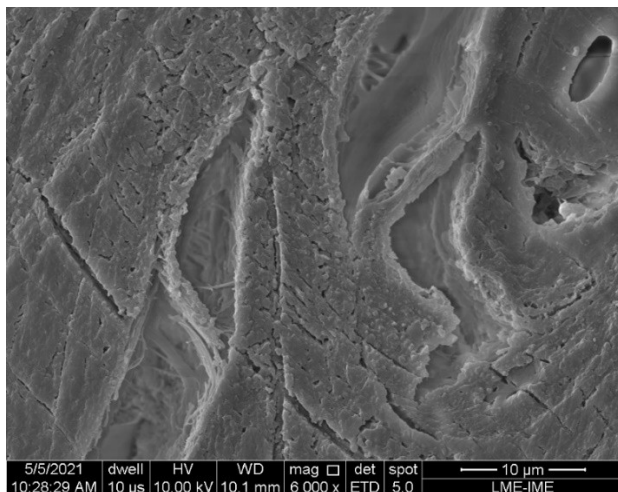
Similarly to what has been reported in previous studies for other hooves, a variation in the diameter of the tubules was identified along the hoof wall. Figure 8 shows a micrograph of a tubule observed in the distal region of the wall, with a diameter of 33.52  $\mu\text{m}$ . In addition to the variation in diameter compared to the tubule in the intermediate region, a variation in shape can be seen, which is more spherical in the case of the distal region. These values are within the range of diameters found in the literature, which vary from 10 to 60  $\mu\text{m}$ , if we consider the diameter of the outer layer of the tubule [14,29-31].

Figure 9 shows a micrograph of the region exactly adjacent to the one shown in 8. This figure shows the fibrils of the inner keratin cell layers, separated by the propagation of a crack. It is believed that the presence of this layered structure, with a well-defined interface between the cells, is related to a greater capacity for stress transfer and energy absorption [14]. This is due to the delamination, elongation and rupture mechanisms of the keratin fibrils present in the intertubular material [5].

**Fig. 8** - Micrograph of a single tubule in cross-section of the wall in the distal region, showing the measured diameter



**Fig. 9** - Micrograph of the cross-section of the hoof wall in the intermediate region, showing a crack and the IFs in the inner layers.



## 4. Conclusion

The samples extracted from the abaxial wall of bovine hooves had their structure and composition assessed using water absorption and moisture content tests, X-ray diffraction (XRD), Fourier transform infrared spectroscopy (FTIR) and scanning electron microscopy (SEM). The following conclusions were reached:

- In both regions studied (*i.e.* distal and proximal), the percentage by weight of water absorbed approaches a plateau after 3 days of immersion. This may indicate that an immersion interval of 4 days is sufficient to ensure total hydration of the hoof wall. In addition, no significant differences were observed in the water absorption of the different regions studied, but the moisture content after immersion was higher for the proximal region, similar to that reported for equine hooves.
- X-ray diffraction analysis showed the periodicity associated with the  $\alpha$ -helix molecules of hoof keratin. Interpretation of the observed spacings showed that there was no significant difference between the outer and inner walls in the distal region, and there was a difference between the distal and proximal regions, with the spacing being smaller in the proximal region. Furthermore, in both regions, as the moisture content of the samples increased, there was a reduction in the observed spacings, which may be indicative of the interaction of water molecules with the  $\alpha$ -helix structure of the keratin.
- Fourier transform infrared spectroscopy (FTIR) analysis enabled the identification of various absorption bands related to the chemical structures of amides A, I, II and III present in the  $\alpha$ -keratins. In addition, varying the moisture content of the samples did not reveal any shift in the observed bands, only a change in the relative intensity of the bands.
- By observing the cross-section of the hoof wall in different areas, the internal structure of this material could be seen. Tubules of different shapes, from spherical to oval, and sizes, from 6 to 33  $\mu\text{m}$ , could be identified in the structure. In addition,

four distinct zones were identified and compared to what has been reported in previous studies. It is believed that these zones, with IFs in different orientations, may contribute to greater energy absorption in the hoof wall.

## Acknowledgments

The authors would like to thank IME for the resources used to carry out this work, as well as financing from CNPq, CAPES and FAPERJ.

## References

- [1] MCKITTRICK, J.; CHEN, P. Y.; TOMBOLATO, L.; NOVITSKAYA, E. E.; TRIM, M. W.; HIRATA, G. A.; OLEVSKY, E. A.; HORSTEMEYER, M. F.; MEYERS, M. A. Energy Absorbent Natural Materials and Bioinspired Design Strategies: A Review. *Materials Science Engineering C*, v. 30, p. 331-342, 2010.
- [2] MEYERS, M. A.; CHEN, P. Y. *Biological Materials Science*. Nova York: Cambridge University Press, 2014.
- [3] MCKITTRICK, J.; CHEN, P. Y.; BODDE, S. G.; YANG, W.; NOVITSKAYA, E. E.; MEYERS, M. A. The Structure, Functions, and Mechanical Properties of Keratin. *JOM*, v. 64, p. 449-468, 2012.
- [4] WANG, B.; YANG, W.; MCKITTRICK, J.; MEYERS, M. A. Keratin: Structure, Mechanical Properties, Occurrence in Biological Organisms, and Efforts at Bioinspiration. *Progress in Materials Science*, v. 76, p. 229-318, 2016.
- [5] LAZARUS, B. S.; VELASCO-HOGAN, A.; GÓMEZ-DEL RÍO, T.; MEYERS, M. A.; JASIUK, I. A Review of Impact Resistant Biological and Bioinspired Materials and Structures. *Journal of Materials Research and Technology*. v. 9, p. 15705-15738, 2020
- [6] FEUGHELMAN, M. *Mechanical Properties and Structure of Alpha-Keratin Fibres: Wool, Human Hair and Related Fibres*. Sydney: UNSW Press, 1997.
- [7] FRASER, R. D.; MACRAE, T. P. Molecular Structure and Mechanical Properties of Keratins. *Symposia of the Society for Experimental Biology*, v. 34, p. 211-246, 1980.
- [8] FRASER, R. D. B.; MACRAE, T. P.; ROGERS, G. E. *Keratins: Their Composition, Structure and Biosynthesis*, Charles C. Thomas. Springfield: [S. n], 1972.
- [9] BERTRAM, J. E.; GOSLINE, J. M. Functional Design of Horse Hoof Keratin: The Modulation of Mechanical Properties through Hydration Effects. *The Journal of Experimental Biology*, v. 130, p. 121-136, 1987.
- [10] FEUGHELMAN, M.; ROBINSON, M. S. The Relationship Between Some Mechanical Properties of Single Wool Fibers and Relative Humidity. *Textile Research Journal*, v. 37, p. 441-446, 1967.
- [11] HUANG, W.; YARAGHI, N. A.; YANG, W.; VELAZQUEZ-OLIVERA, A., LI, Z.; RITCHIE, R. O.; KISAILUS, D.; STOVER, S. M., MCKITTRICK, J. A Natural Energy Absorbent Polymer Composite: The Equine Hoof Wall. *Acta Biomaterialia*, v. 90, p. 267-277, 2019.
- [12] TOMBOLATO, L.; NOVITSKAYA, E. E.; CHEN, P. Y.; SHEPPARD, F. A.; MCKITTRICK, J. Microstructure, Elastic Properties and Deformation Mechanisms of Horn Keratin. *Acta Biomaterialia*, v. 6, p. 319-330, 2010.
- [13] ZHANG, Q.; BIN, Li, C.; PAN, Y. T.; SHAN, G. H.; CAO, P.; HE, J.; LIN, Z. S.; AO, N. J.; HUANG, Y. X. Microstructure and Mechanical Properties of Horns Derived from Three Domestic Bovines. *Materials Science and Engineering C*, v. 33, p. 5036-5043, 2013.
- [14] WANG, B.; ZHOU, B.; ZHANG, X.; WANG, B. Microstructure and Mechanical Properties of an Alpha Keratin Bovine Hoof Wall. *Journal of Mechanical Behavior of Biomedical Materials*, v. 104, 103689, 2020.
- [15] CLARK, C.; PETRIE, L. Fracture Toughness of Bovine Claw Horn from Cattle with and without Vertical Fissures. *The Veterinary Journal*, v. 173, p. 541-547, 2007.
- [16] BAILLIE, C.; SOUTHAM, C.; BUXTON, A.; PAVAN, P. Structure and Properties of Bovine Hoof Horn. *Advanced Composites Letters*. Journal, v. 9, 2000.
- [17] ASTM D570-98 Standard Test Method for Water Absorption of Plastics, 2018.
- [18] WU, M.; SHEN, S.; YANG, X.; TANG, R. Preparation and Study on the Structure of Keratin/PVA Membrane Containing Wool Fibers. *IOP Conference Series: Materials Science and Engineering*, v. 254, 2017.
- [19] VALKOV, A.; ZINIGRAD, M.; SOBOLEV, A.; NISNEVITCH, M. Keratin Biomembranes as a Model for Studying Onychomycosis. *International Journal Molecular Science*, v. 21, 2020.
- [20] KASAPI, M. A.; GOSLINE, J. M. Exploring the Possible Functions of Equine Hoof Wall Tubules. *Equine Veterinary Journal*, v. 30, p. 10-14, 2010.

- [21] KITCHENER, A. Effect of Water on the Linear Viscoelasticity of Horn Sheath Keratin. *Journal Mater Science Letterring*, v. 6, p. 321-322, 1987.
- [22] COLLINS, S. N.; COPE, B. C.; HOPEGOOD, L.; LATHAM, R. J.; LINFORD, R. G. Stiffness as a Function of Moisture Content in Natural Materials : Characterisation of Hoof Horn Samples. *Journal Mater Science*, v. 33, p. 5185-5191, 1998.
- [23] FRASER, R. D. B.; MACRAE, T. P. The Structure of  $\alpha$ -Keratin. *Polymer (Guildf)*, v. 14, p. 61-67, 1973.
- [24] KUI, H.; LIU, X.; LIU, J.; LIANG, W.; ZHANG, S.; QIAN, Z.; REN, L. The Passive Contact Stability of Blue Sheep Hoof Based on Structure, Mechanical Properties, and Surface Morphology. *Frontiers in Bioengineering and Biotechnology*, v. 8, p. 1-16, 2020.
- [25] HUANG, W. Impact Resistant and Energy Absorbent Natural Keratin Materials: Horns and Hooves: [S. n.], 2018.
- [26] PARKER, F. S. Amides and Amines. In *Applications of Infrared Spectroscopy in Biochemistry, Biology, and Medicine*. Boston: Springer, 1971. p. 165-172.
- [27] KUMAR, S. L.; ANANDHAVELU, S.; SWATHY, M. Preparation and Characterization of Goat Hoof Keratin/ Gelatin/Sodium Alginate Base Biofilm for Tissue Engineering Application. *Integrated Ferroelectrics*, v. 202, p. 1-12, 2019.
- [28] VERMUNT, J. J.; GREENOUGH, P. R. Structural Characteristics of the Bovine Claw: Horn Growth and Wear, Horn Hardness and Claw Conformation. *British Veterinary Journal*, v. 151, p. 157-180, 1995.
- [29] FRANCK, A.; COCQUYT, G.; SIMOENS, P.; DE BELIE, N. Biomechanical Properties of Bovine Claw Horn. *Biosystem Engineer*, v. 93, p. 459-467, 2006.
- [30] WANG, B.; HUANG, Y.; ZHOU, B.; LI, W.; CHEN, H. Nanoindentation and Hierarchy Structure of the Bovine Hoof Wall. *Materials (Basel)*, v. 14, 2021.
- [31] ASSIS, B. M.; SILVA, L. A. F.; LIMA, C. R. O.; GOUVEIA, R. F.; VULCANI, V. A. S.; DE SANT'ANA, F. J. F.; RABELO, R. E. Microstructure and Hardness of Buffalo's Hoofs. *Anatomia Histologia Embryologia*, v. 46, p. 439-445, 2017.